

Vibration and stability of initially stressed sandwich plates with FGM face sheets in thermal environments

Chun-Sheng Chen¹, Fwu-Hsing Liu¹ and Wei-Ren Chen^{*1,2}

¹Department of Mechanical Engineering, Lunghwa University of Science and Technology, Guishan Shiang, Taoyuan, 33306, Taiwan

²Department of Mechanical Engineering, Chinese Culture University, Taipei 11114, Taiwan

(Received January 18, 2015, Revised November 26, 2016, Accepted December 29, 2016)

Abstract. In this paper, thermal effect on the vibration and stability of initially stressed sandwich plates with functionally graded material (FGM) face sheets is analyzed. Material properties of FGM face sheet are graded continuously in the thickness direction. The variation of FGM properties assumes a simple power law distribution in terms of the volume fractions of the constituents. The governing equations of arbitrarily initially-stressed sandwich plates including the effects of transverse shear deformation and rotary inertia are derived. The initial stress is taken to be a combination of a uniaxial extensional stress and a pure bending stress in the examples. The eigenvalue problems are formed to study the vibration and buckling characteristics of simple supported initially stressed FGM/metal/FGM plates. The effects of volume fraction index, temperature rise, initial stress and layer thickness of metal on the natural frequencies and buckling loads are investigated. The results reveal that the volume fraction index, initial stresses and layer thickness of metal have significant influence on the vibration and stability of sandwich plates with FGM face sheets.

Keywords: thermal effect; sandwich plate; FGM face sheet; volume fraction index; initial stress

1. Introduction

The lightweight composite structures have been increasingly used in many engineering constructions for the past years. The advanced composite materials, metal-ceramic functionally graded materials (FGMs), have attracted much attention in spacecraft and engineering industries due to their high temperature resistance and toughness properties. Basically, FGMs are microscopically inhomogeneous and their mechanical properties smoothly and continuously vary in a structure. Unlike traditional laminated composites that have a mismatch of properties across the interface of two bonded layers, which may result in delaminating under high-temperature operation conditions, FGMs can be used in a high-temperature environment wherein the ceramics contribute a significant heat-resistant ability to FGMs while the metals keep a certain extent of toughness (Zhao *et al.* 2009, Shafiee *et al.* 2014). These special characteristics make them preferable to other engineering materials while used as heat-resistant materials for engineering structures at high temperature environments. It is well known that the temperature rise has a significant influence on the vibration and stability behaviors of plates subject to high temperature. Hence, the vibration and stability behaviors of plates made of FGMs subjected to high temperature conditions should be clearly described in order to use the FGMs appropriately.

The vibration and buckling of functionally grade plates (FGPs) in thermal environments have received researchers' great attention for many years. The buckling analysis of FGPs under three types of mechanical loads and two types of thermal loads was presented by Shariat and Eslami (2007). The equilibrium and stability equations were derived based on the third plate theory and used to obtain the critical buckling loads. The free vibration of FGPs in thermal environments was studied by Li *et al.* (2009). The natural frequencies were obtained by Ritz method. Parametric study was conducted for temperature fields, boundary conditions and volume fraction indices of FGPs. The effects of the material constitutions of FG panels on thermal buckling and flutter characteristics were examined. The thermal buckling of FGPs with circular holes at the center was investigated by Zhao *et al.* (2009) based on the first order plate theory. The effects of the volume fraction index and geometry of hole on the thermal buckling of FGPs were studied. A higher order deformation theory was utilized to analyze the thermal buckling of FGPs by Matsunaga (2009). Several approximate theories were applied to solve the eigenvalue problems of simply supported FGPs. Critical temperatures were obtained for FGPs under uniformly and linearly distributed temperatures across the plate thickness. The vibration analysis of functionally graded annular plates subjected to thermal environment was presented by Malekzadeh *et al.* (2010). The initial thermal stresses were obtained by the 3D thermoelastic equilibrium equations. Both the thermoelastic equilibrium and free vibration equations were solved by the differential quadrature method. The influences of temperature rise, material and geometric parameters on the

*Corresponding author, Professor,
E-mail: wrchen@faculty.pccu.edu.tw

natural frequencies were studied. The vibration and buckling behavior of curved shell panels made of FGMs was investigated by Pradyumna and Bandyopadhyay (2010). The shell panels were under a temperature field and they were also subjected to a uniaxial compressive load in the buckling analysis. The properties of FGMs were assumed to vary across the thickness direction according to a simple power law distribution. The effects of geometric properties, material constituents, and restraint conditions on the vibration and buckling were discussed.

The thermal buckling analysis of thin FGPs under the thermal loads of uniform and nonlinear temperature rise through the thickness was studied by Kazerouni *et al.* (2010). The stability equations coupled in terms of in-plane and out-of plane displacements were derived using the classical plate theory and principle of minimum potential energy. The effects of aspect ratio, thickness to side ratio, volume fraction index and boundary conditions on the critical buckling temperature of FGPs were investigated. The buckling and postbuckling behavior of simply supported functionally graded nanotube-reinforced composite plates subjected to uniaxial compression in thermal environments was investigated by Shen and Zhu (2010). The results revealed that the functionally graded nanotube reinforcement significantly increases the buckling postbuckling loads of the plates, and that the carbon nanotube volume fraction has a major impact on the buckling load and postbuckling behavior. The vibration analysis of FGPs with mixed boundary conditions in thermal environment was dealt with by Shi and Dong (2012) using the 3D elasticity theory and the Chebyshev–Ritz method. The upper and lower surfaces and inner and outer sides were assumed to be partially fixed. The influences of various mixed boundary conditions, the temperature rise, the material graded index and the geometrical parameters on the eigenfrequencies were investigated. Based on the classical plate theory, the buckling behavior of rectangular FGPs under thermal loadings was analyzed by Ghannadpour *et al.* (2012) using a finite strip method. The functionally graded material properties were assumed to vary continuously across the plate thickness according to the simple power law distribution. The solution was found by minimizing the total potential energy and solving the eigenvalue problem. The effects of geometrical and material properties on the FGPs' buckling temperature difference were investigated. The free vibration behavior of rectangular exponential FGPs under various boundary conditions was presented by Chakravarty and Pradhan (2014). The eigenfrequency equation was obtained by the Rayleigh-Ritz method to study the effects of constituent volume fractions and aspect ratios on the natural frequencies.

The free flexural vibration of FGPs with a through center crack in thermal environment was studied by Natarajan *et al.* (2011) based on first order shear deformation theory. The shear correction factors were calculated by the energy equivalence principle. The effects of the crack length, aspect ratio, skew angle, temperature, thickness and boundary conditions on the natural frequency of plates were investigated. The vibration behavior of FGPs with cutouts and cracks in thermal environment was studied by

Rahimabadi *et al.* (2013) based on the first order shear deformation theory. The effective properties of the FGM were estimated based on the Mori-Tanaka homogenization scheme. The effects of the plate geometry, the cutout geometry, the crack length, the thermal gradient and the boundary conditions on the natural frequencies were discussed. The free vibration of sandwich plates with FGM face sheets in different thermal environments was analyzed by Khalili and Mohammadi (2012) using an improved high-order sandwich plate theory. The governing vibration equations of motion were established based on the Hamilton's principle. The results indicated that the variation of the side-to-thickness ratio, the core-to-face sheet thickness ratio and the temperature has a significant effect on the fundamental frequency. The static and free vibration of functionally graded sandwich plates with piezoelectric skins were investigated by Loja *et al.* (2013) using various shear deformation theories. The effective properties of FGMs were estimated using the Mori-Tanaka homogenization scheme.

All previous studies on FGPs were limited to the condition that the plates were not subjected to any initial stresses. Meanwhile, thermal effect on the vibration and stability of sandwich plates with FGM face sheets have seldom been reported in the literature. Residual stresses caused by manufacture processes can often be found in the structures made of FGMs, which may significantly affect the vibration and stability behaviors of the structures. Therefore, the study of vibration of FGPs including the sensitivity of initial stresses is necessary. The free vibration of FGPs made of ceramic and metal under initial thermal stresses was presented by Mahi *et al.* (2013) based on higher order shear deformation plate theory. Natural frequencies were computed based on the Ritz method. The vibration of initially stressed functionally graded plates without thermal effect had been carried out by the authors of this study (Chen *et al.* 2006, 2008, 2009). However, there has been no study considering the effect of an arbitrary initial stress on the vibration and stability of sandwich plates with FGM face sheets in thermal environments. In the present paper, the governing equations of sandwich plates with FGM face sheets subjected to non-uniform initial stresses are derived, and an example of a simply supported FGM/metal/FGM plate subjected to an initial stress is solved. The material property distribution is presented by a simple power law in the volume fraction of ceramic material in this study and the initial stress is a combination of a pure bending stress and an extensional stress. Finally, the effect of initial stress and other factors on vibration and stability problems is investigated.

2. Modeling of functionally graded materials

In the present study, the FGM/metal/FGM sandwich plate considered is shown schematically in Fig. 1. The material of its top and bottom face sheet is FGM and that of the core is a metal. The total thickness of FGM/metal/FGM plate is h . The thickness of the top FGM sheet layer, middle metal layer and bottom FGM sheet layer is $t_{TG} = (z_1 - z_2)$, $t_M = (z_2 - z_3)$ and $t_{BG} = (z_3 - z_4)$, respectively. Here, the FGM

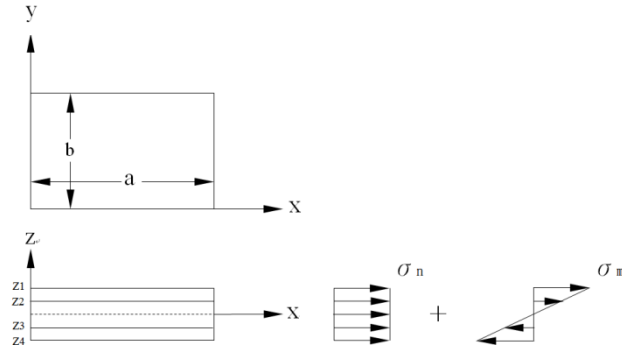


Fig. 1 Configuration of FGM/metal/FGM sandwich plate and the applied stress field

sheet is made from a mixture of ceramic and metal.

It is assumed that the properties of FGM of the sandwich plate vary along its thickness according to a simple power law of the constituents' volume fractions. Thus, the effective material properties P_F of FGM with two constituents, can be expressed as

$$P_F = P_C V_C + P_M V_M \quad (1)$$

where P_C and P_M represent the properties of the ceramic and metal material, respectively; V_C and V_M denote the volume fractions of the ceramic and metal material and are related by

$$V_C + V_M = 1 \quad (2)$$

Because the volume fraction is assumed to vary across the thickness of the plate according to a simple power law, the volume fraction V_M of the top FGM face sheet assumes the following form

$$V_M = \left(\frac{z - z_1}{z_2 - z_1} \right)^n \quad (3)$$

and the volume fraction V_M of the bottom FGM face sheet is expressed as

$$V_M = \left(\frac{z - z_4}{z_3 - z_4} \right)^n \quad (4)$$

Here n is the volume fraction index of which value is taken to be positive ($0 \leq n \leq \infty$). By introducing Eqs. (2)-(4) into Eq. (1), the effective material properties of the respective top and bottom FGM face sheet can be obtained as (Yang and Shen 2003, Shen and Li 2008).

$$P_F(z) = (P_M - P_C) \left(\frac{z - z_1}{z_2 - z_1} \right)^n + P_C \quad (z_2 < z \leq z_1) \quad (5)$$

$$P_F(z) = (P_M - P_C) \left(\frac{z - z_4}{z_3 - z_4} \right)^n + P_C \quad (z_4 \leq z < z_3) \quad (6)$$

From Eqs. (5) and (6), the effective material properties such as Young's modulus E , Poisson's ratio ν , mass density

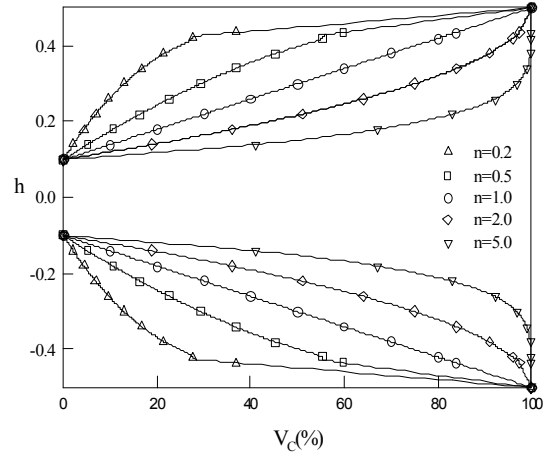


Fig. 2 Variation of ceramic volume fraction through the thickness of FGM/metal/FGM sandwich plates

ρ , thermal expansion coefficient α and thermal conductivity κ at any position can be determined. The variation of ceramic volume fraction of a typical FGM/metal/FGM sandwich plate with $t_M = 0.2h$ and $t_{TG} = t_{BG}$ for the various volume fraction index is shown in Fig. 2. The x-axis of the figure stands for the volumetric percentage of ceramic while the y-axis represents the position along the thickness of sandwich plate. The volume fraction index n is set to be 0.2, 0.5, 1, 2 and 5. As can be seen, the outer surface of the top and bottom FGM face sheet is ceramic-rich and the interface between FGM face sheet and metal core is metal-rich. Hence, the upper and lower surfaces of the FGM/metal/FGM sandwich plate are ceramic-rich. The larger volume fraction index indicates a rapid increase in the volume fraction of ceramic along the thickness of FGM face sheet.

For FGM/metal/FGM plates subjected to temperature change across the thickness, the nonuniform temperature field is assumed to vary only along the thickness direction due to heat conduction. The temperature distribution $T(z)$ through the thickness is governed by the one dimensional steady state heat conduction equation

$$\frac{d}{dz} \left[\kappa(z) \frac{dT(z)}{dz} \right] = 0 \quad (7)$$

where

$$\kappa(z) = \begin{cases} \kappa_F(z) & z_2 \leq z \leq z_1 \\ \kappa_M(z) & z_3 < z < z_2 \\ \kappa_F(z) & z_4 \leq z \leq z_3 \end{cases}$$

and

$$T(z) = \begin{cases} T_T(z) & z_2 \leq z \leq z_1 \\ T_M(z) & z_3 < z < z_2 \\ T_B(z) & z_4 \leq z \leq z_3 \end{cases}$$

T_T , T_M and T_B represent the temperature change along the top FGM face sheet, metal core and bottom FGM face sheet, respectively. The temperature at $z = z_1, z_2, z_3$ and z_4 is denoted as T_1, T_2, T_3 and T_4 , respectively. The continuity

conditions at $z = z_2$ and z_3 are

$$\begin{aligned} T_T(z_2) = T_M(z_2) = T_2, \quad T_M(z_3) = T_B(z_3) = T_3, \\ \kappa_F \frac{dT_T}{dz} \Big|_{z=z_2} = \kappa_M \frac{dT_M}{dz} \Big|_{z=z_2}, \quad \kappa_M \frac{dT_M}{dz} \Big|_{z=z_3} = \kappa_F \frac{dT_B}{dz} \Big|_{z=z_3} \end{aligned} \quad (8)$$

From Eqs. (7) and (8), the solution of Eq. (7) can be determined by the use of polynomial series. By taking the first six terms of the series, the nonuniform temperature fields of the top FGM face sheet, metal core and bottom FGM face sheet of sandwich plate are given as follows

$$T_T(z) = T_1 + (T_2 - T_1)\eta_T(z)$$

$$T_M(z) = [T_3z_2 - T_2z_3 + (T_2 - T_3)z]/(z_2 - z_3) \quad (9)$$

$$T_B(z) = T_4 + (T_3 - T_4)\eta_B(z)$$

$$\text{where } \eta_T(z) = \frac{1}{C_1} \sum_{i=0}^5 (-1)^i \frac{(\kappa_M - \kappa_C)^i}{(i \times n + 1)\kappa_C^i} \left(\frac{z - z_1}{z_2 - z_1}\right)^{i \times n + 1}$$

$$\eta_B(z) = \frac{1}{C_1} \sum_{i=0}^5 (-1)^i \frac{(\kappa_M - \kappa_C)^i}{(i \times n + 1)\kappa_C^i} \left(\frac{z - z_4}{z_3 - z_4}\right)^{i \times n + 1}$$

$$T_2 = \frac{[\kappa_M/(z_2 - z_3) + (\kappa_M C_2/(z_1 - z_2)C_1)]T_1 + T_4 \kappa_M/(z_2 - z_3)}{\kappa_M C_2/(z_1 - z_2)C_1 + 2\kappa_M/(z_2 - z_3)}$$

$$T_3 = \frac{[\kappa_M/(z_2 - z_3) + (\kappa_M C_2/(z_3 - z_4)C_1)]T_4 + T_1 \kappa_M/(z_2 - z_3)}{\kappa_M C_2/(z_3 - z_4)C_1 + 2\kappa_M/(z_2 - z_3)}$$

$$C_1 = \sum_{i=0}^5 (-1)^i \frac{(\kappa_M - \kappa_C)^i}{(i \times n + 1)\kappa_C^i},$$

$$C_2 = \sum_{i=0}^5 (-1)^i \frac{(\kappa_M - \kappa_C)^i}{\kappa_C^i}$$

3. Problem formulation

The governing equations for a FGM/metal/FGM sandwich plat subjected to the arbitrary initial stress and thermal loading are established by applying the Hamilton's principle. The transverse shear deformation effect is considered in deriving the governing equations. It is similar to the technique described by Brunell and Robertson (1974) and Chen *et al.* (2009). In order to obtain the governing equations, the Hamilton's principle is written as

$$\int_{t_0}^{t_1} (\delta U_s - \delta K_t - \delta W_e - \delta W_i) dt = 0 \quad (10)$$

where U_s , K_t , W_e and W_i is the strain energy, kinetic energy, work of external forces and work of internal forces, respectively; t_0 and t_1 are two arbitrary times. The energy variations can be given as follows

$$\delta U_s = \int_{V_0} \sigma_{ij} \delta \varepsilon_{ij} dV \quad \delta K_t = \int_{V_0} \rho \dot{v}_i \delta \dot{v}_i dV$$

$$\delta W_e = \int_{S_0} p_i \delta v_i dS \quad \delta W_i = \int_{V_0} X_i \delta v_i dV$$

Here δ denotes the variational operator; σ_{ij} and ε_{ij} represent the stress and strain in the material coordinates, respectively; v_i is the displacement in the spatial frame; p_i is the surface force per unit area; X_i is the body force per unit initial volume; V_0 and S_0 are the volume and boundary surface, respectively. Then introducing the energy variations of U_s , K_t , W_e and W_i into Eq. (10) yields

$$\int_{t_0}^{t_1} \left[\int_{V_0} (\sigma_{ij} \delta \varepsilon_{ij} - X_i \delta v_i - \rho \dot{v}_i \delta \dot{v}_i) dV - \int_{S_0} (p_i \delta v_i) dS \right] dt = 0 \quad (11)$$

Based on the first order plate theory, the displacement fields assume the following forms

$$v_x(x, y, z, t) = u_x(x, y, t) + z\varphi_x(x, y, t)$$

$$v_y(x, y, z, t) = u_y(x, y, t) + z\varphi_y(x, y, t) \quad (12)$$

$$v_z(x, y, z, t) = w(x, y, t)$$

where u_x , u_y and w are the displacements of the middle surface in the x , y and z direction, respectively; φ_x and φ_y denotes the rotation angle about y and x axis, respectively. The two edges of the rectangular plate are set along x and y axes, respectively. The constitutive relations for the plate including the thermal effect can be written as

$$\begin{bmatrix} \sigma_{xx} \\ \sigma_{yy} \\ \sigma_{yz} \\ \sigma_{zx} \\ \sigma_{xy} \end{bmatrix} = \begin{bmatrix} C_{11} & C_{12} & 0 & 0 & 0 \\ C_{12} & C_{22} & 0 & 0 & 0 \\ 0 & 0 & C_{44} & 0 & 0 \\ 0 & 0 & 0 & C_{55} & 0 \\ 0 & 0 & 0 & 0 & C_{66} \end{bmatrix} \begin{bmatrix} \varepsilon_{xx} - \alpha \Delta T \\ \varepsilon_{yy} - \alpha \Delta T \\ \varepsilon_{yz} \\ \varepsilon_{zx} \\ \varepsilon_{xy} \end{bmatrix} \quad (13)$$

And the stress-displacement relations are found to be

$$\sigma_{xx} = C_{11}(u_{,xx} + z\varphi_{,xx} - \alpha \Delta T) + C_{12}(u_{,yy} + z\varphi_{,yy} - \alpha \Delta T)$$

$$\sigma_{yy} = C_{12}(u_{,xx} + z\varphi_{,xx} - \alpha \Delta T) + C_{22}(u_{,yy} + z\varphi_{,yy} - \alpha \Delta T)$$

$$\sigma_{yz} = C_{44}(\varphi_y + w_{,y}) \quad (14)$$

$$\sigma_{zx} = C_{55}(\varphi_x + w_{,x})$$

$$\sigma_{xy} = C_{66}(u_{,xy} + z\varphi_{,xy} + u_{,yx} + z\varphi_{,yx})$$

Substitute Eqs. (12)-(14) into Eq. (11), perform all necessary partial integrations and collect terms together by the displacement variation to yield the following governing equations

$$\begin{aligned} [A_{11}u_{,xx} + A_{12}u_{,yy} + N_{xx}u_{,xx} + M_{xx}\varphi_{,xx} + N_{xx}^T u_{,xx} \\ + M_{xx}^T \varphi_{,xx} + N_{xy}u_{,xy} + M_{xy}\varphi_{,xy} + N_{xz}u_{,z,x}]_{,x} \\ [A_{66}(u_{,xy} + u_{,yx}) + N_{yy}u_{,xy} + M_{yy}\varphi_{,xy} + N_{yy}^T u_{,xy} \\ + M_{yy}^T \varphi_{,xy} + N_{xy}u_{,xx} + M_{xy}\varphi_{,xx} + N_{yz}u_{,z,y}]_{,y} \\ + f_x = I_1 \ddot{u}_x \end{aligned} \quad (15)$$

$$\begin{aligned}
 & [A_{66}(u_{x,y} + u_{y,x}) + N_{yy}u_{y,x} + M_{yy}\varphi_{y,x} + N_{xx}^T u_{y,x} \\
 & + M_{xx}^T \varphi_{y,x} + N_{xy}u_{y,y} + M_{xy}\varphi_{y,y} + N_{xz}u_{z,y}]_{,x} \\
 & + [A_{12}u_{x,x} + A_{22}u_{y,y} + N_{yy}u_{y,y} + M_{yy}\varphi_{y,y} + N_{yy}^T u_{y,y} \\
 & + M_{yy}^T \varphi_{y,y} + N_{xy}u_{y,x} + M_{xy}\varphi_{y,x} + N_{xz}u_{z,y}]_{,y} \\
 & + f_y = I_1 \ddot{u}_y
 \end{aligned} \quad (16)$$

$$\begin{aligned}
 & [A_{55}(w_x + \varphi_x) + N_{xx}w_x + N_{xx}^T w_x + N_{xy}w_x]_{,x} \\
 & + [A_{44}(w_y + \varphi_y) + N_{xy}w_x + N_{yy}w_y + N_{yy}^T w_y]_{,y} \\
 & + f_z = I_1 \ddot{w}
 \end{aligned} \quad (17)$$

$$\begin{aligned}
 & [D_{11}\varphi_{x,x} + D_{12}\varphi_{y,y} + M_{xx}u_{x,x} + M_{xx}^* \varphi_{x,x} + M_{xx}^T u_{x,x} \\
 & + M_{yy}^{T*} \varphi_{x,x} + M_{xy}u_{x,y} + M_{xz}u_{z,x} + M_{xy}^* \varphi_{x,y}]_{,x} \\
 & + [D_{66}(\varphi_{x,y} + \varphi_{y,x}) + M_{yy}u_{x,y} + M_{yy}^* \varphi_{x,y} + M_{yy}^T u_{x,y} \\
 & + M_{yy}^{T*} \varphi_{x,y} + M_{xy}u_{x,x} + M_{xy}^* \varphi_{x,x} + M_{yz}u_{z,x}]_{,y} \\
 & - A_{55}(w_x + \varphi_x) - (N_{xz}u_{x,x} + M_{xz}\varphi_{x,x} + N_{zz}\varphi_x \\
 & + N_{zy}u_{x,y} + M_{zy}\varphi_{x,y}) + m_x = I_3 \ddot{\varphi}_x
 \end{aligned} \quad (18)$$

$$\begin{aligned}
 & [D_{66}(\varphi_{x,y} + \varphi_{y,x}) + M_{xx}u_{y,x} + M_{xx}^* \varphi_{y,x} + M_{xx}^T u_{y,x} \\
 & + M_{xx}^{T*} \varphi_{y,x} + M_{xy}u_{y,y} + M_{xz}u_{z,x} + M_{xy}^* \varphi_{y,y}]_{,x} \\
 & + [D_{12}\varphi_{x,x} + D_{22}\varphi_{y,y} + M_{yy}u_{y,y} + M_{yy}^* \varphi_{y,y} + M_{yy}^T u_{y,y} \\
 & + M_{yy}^{T*} \varphi_{y,y} + M_{xy}\varphi_{y,x} + M_{xy}^* u_{y,x} + M_{xz}u_{z,y}]_{,y} \\
 & - A_{44}(w_y + \varphi_y) - (N_{xz}u_{y,x} + M_{xz}\varphi_{y,x} + N_{zz}\varphi_y \\
 & + N_{zy}u_{y,y} + M_{zy}\varphi_{y,y}) + m_y = I_3 \ddot{\varphi}_y
 \end{aligned} \quad (19)$$

in which f_x, f_y, f_z, m_x and m_y are the lateral loadings. The other coefficients related to the material parameters, initial stress resultants, thermal stress resultants and rotary inertia are defined as follows

$$(A_{ij}, D_{ij}) = \int C_{ij}(1, z^2) dz \quad (i, j = 1, 2, 4, 5, 6)$$

$$(N_{ij}, M_{ij}, M_{ij}^*) = \int \sigma_{ij}(1, z, z^2) dz \quad (i, j = x, y, z)$$

$$(M_{ii}^T, M_{ii}^T, M_{ii}^{T*}) = \int \alpha E \Delta T / (1 - \nu)(1, z, z^2) dz \quad (i, j = x, y)$$

$$(I_1, I_3) = \int \rho(z)(1, z^2) dz$$

where all the integrals are integrated through the thickness h of the plate from $-h/2$ to $h/2$.

4. Eigenvalue problems

In the present study, the initially-stressed FGM/metal/FGM plate of concern can be regarded as a three-layered laminate plate which is similar to a sandwich plate. The top layer, core layer and bottom layer of the sandwich plate are made of FGM, metal and FGM, respectively. There are so many parameters can be varied in the governing Eqs. (15)-(19) so it is intricate to present results for all cases. Thus, only a few typical cases will be selected for discussion.

Only the simply supported initially-stressed FGM/metal/FGM plate in thermal environments is considered. The lateral loads and body forces are taken to be zero and the nonzero initial stresses is assumed to be

$$\sigma_{xx} = \sigma_n + 2z\sigma_m / h \quad (20)$$

which is a combination of a constant extensionally normal stress σ_n and bending stress σ_m . The only nonzero initial stress resultants are $N_{xx} = h\sigma_n$, $M_{xx} = \beta h^2 \sigma_n / 6$ and $M_{xx}^* = h^3 \sigma_n / 12$. Here β is the ratio of bending stress to normal stress, σ_m / σ_n , and when $\beta = 0$ there is no initial bending stress.

For the simply supported FGM/metal/FGM plate, the displacement fields satisfying the geometric boundary conditions assume the following form

$$\begin{aligned}
 u_x &= \sum \sum h U_{mn} \cos(m\pi x/a) \sin(n\pi y/b) e^{i\sigma_{mn}t} \\
 u_y &= \sum \sum h V_{mn} \sin(m\pi x/a) \sin(n\pi y/b) e^{i\sigma_{mn}t} \\
 w &= \sum \sum h W_{mn} \sin(m\pi x/a) \sin(n\pi y/b) e^{i\sigma_{mn}t} \\
 \varphi_x &= \sum \sum \Psi_{xmn} \cos(m\pi x/a) \sin(n\pi y/b) e^{i\sigma_{mn}t} \\
 \varphi_y &= \sum \sum \Psi_{ymn} \sin(m\pi x/a) \cos(n\pi y/b) e^{i\sigma_{mn}t}
 \end{aligned} \quad (21)$$

All summations are summed up from $m, n = 1$ to ∞ . $e^{i\sigma_{mn}t}$ will be neglected in Eq. (21) while a buckling problem is concerned. Substituting Eqs. (20) and (21) into Eqs. (15)-(19), and grouping the coefficients for any fixed values of m and n yields the following equation

$$([C] - \lambda[G])\{\Delta\} = \{0\} \quad (22)$$

$$\{\Delta\} = [U_{mn}, V_{mn}, W_{mn}, \Psi_{xmn}, \Psi_{ymn}]^T$$

The parameter λ denotes the corresponding vibration frequency or buckling coefficient.

For the vibration problems of a sandwich plate with FGM face sheets in thermal environments, the coefficients of the symmetric matrix $[C]$ and $[G]$ of Eq. (22) are expressed as follows

$$C_{1,1} = -(A_{11} + N_{xx})\bar{\alpha}^2 - A_{66}\bar{\beta}^2 + \bar{\alpha}^2 N_{xx}^T + \bar{\beta}^2 N_{yy}^T,$$

$$C_{1,2} = -(A_{12} + A_{66})\bar{\alpha}\bar{\beta}$$

$$C_{1,4} = -(M_{xx}\bar{\alpha}^2 + B_{66}\bar{\beta}^2)/h - \beta_{11}\bar{\alpha}^2/h + \bar{\alpha}^2 M_{xx}^T + \bar{\beta}^2 M_{yy}^T,$$

$$C_{1,5} = -(B_{11} + B_{66})\bar{\alpha}\bar{\beta}/h,$$

$$C_{2,2} = -(A_{66} + N_{xx})\bar{\alpha}^2 - A_{22}\bar{\beta}^2 + \bar{\alpha}^2 N_{xx}^T + \bar{\beta}^2 N_{yy}^T,$$

$$C_{2,4} = C_{1,5},$$

$$C_{2,5} = -[M_{xx}\bar{\alpha}^2 + (B_{66}\bar{\alpha}^2 + B_{22}\bar{\beta}^2)]/h + \bar{\alpha}^2 M_{xx}^T + \bar{\beta}^2 M_{yy}^T,$$

$$C_{3,4} = -A_{55}\bar{\alpha}/h,$$

$$C_{3,3} = -(A_{55} + N_{xx})\bar{\alpha}^2 - A_{44}\bar{\beta}^2 + \bar{\alpha}^2 N_{xx}^T + \bar{\beta}^2 N_{yy}^T,$$

$$C_{3,5} = -A_{44}\bar{\beta}/h,$$

$$C_{4,4} = -(D_{11} + M_{xx}^*)\bar{\alpha}^2 + D_{66}\bar{\beta}^2 + A_{55}] / h^2 \\ + \bar{\alpha}^2 M_{xx}^{T*} + \bar{\beta}^2 M_{xx}^{T*},$$

$$C_{4,5} = -(D_{12} + D_{66})\bar{\alpha}\bar{\beta} / h^2,$$

$$\bar{\alpha} = m\pi / a, \quad \bar{\beta} = n\pi / b$$

$$C_{5,5} = -(D_{66} + M_{xx}^*)\bar{\alpha}^2 + D_{22}\bar{\beta}^2 + A_{44}] / h^2 \\ + \bar{\alpha}^2 M_{xx}^{T*} + \bar{\beta}^2 M_{yy}^{T*},$$

$$G_{1,1} = G_{2,2} = G_{3,3} = -I_1, \quad G_{4,4} = G_{5,5} = -I_3 / h^2$$

For the buckling load problems, the coefficients of the symmetric matrix $[C]$ are obtained by neglecting the initial stress resultant terms in the matrix $[C]$. And the coefficients of the matrix $[G]$ are

$$G_{1,1} = G_{2,2} = G_{3,3} = \bar{\alpha}^2,$$

$$G_{1,4} = G_{2,5} = \beta\bar{\alpha}^2 / 6h,$$

$$G_{4,4} = G_{5,5} = \bar{\alpha}^2 / 12h^2$$

As to the thermal buckling problem, the coefficients of matrix $[C]$ are given by neglecting the thermally-induced stress resultant terms in the stiffness matrix $[C]$ in Eq. (22) and the coefficients of matrix $[G]$ are

Table 1 Comparison of the critical buckling temperature (°C) of a FGP due to heat conduction

n	a/h	Present results	Javaheri and Eslami (2002)
0	10	3187.5	3187.5
	20	891.5	933.0
	40	210.8	202.9
1	10	1953.6	1960.0
	20	500.5	497.9
	40	118.8	115.8
5	10	1463.0	1450.7
	20	381.2	373.5
	40	90.3	86.5
10	10	1467.9	1519.5
	20	375.9	372.2
	40	91.1	85.3

Table 2 Comparison of the critical temperature (°C) of a three-layer cross-ply laminated square plate under uniform temperature rise

a/h	Present results	Matsunaga (2005)
2	0.3371	0.3334
10/3	0.2517	0.2465
4	0.2189	0.2148
5	0.1785	0.1763
20/3	0.1291	0.1294
10	0.0728	0.0746
20	0.0219	0.0230

$$G_{1,1} = G_{2,2} = G_{3,3} = \bar{\alpha}^2 N_{xx}^T + \bar{\beta}^2 N_{yy}^T,$$

$$G_{1,4} = G_{2,5} = \bar{\alpha}^2 M_{xx}^T + \bar{\beta}^2 M_{yy}^T,$$

$$G_{4,4} = G_{5,5} = \bar{\alpha}^2 M_{xx}^{T*} + \bar{\beta}^2 M_{yy}^{T*}$$

5. Results and discussions

The natural frequency and buckling load of FGPs without thermal loads had been studied previously by the first author (Chen 2008, 2009) and was proved to be accurate by comparing the obtained results with the published exact solutions. The calculated critical temperatures of FGP and laminated plates under thermal loadings are presented in Tables 1 and 2, respectively, and compared with the results by Javaheri and Eslami (2002) and Matsunaga (2005). From these comparisons, the results obtained from the present method agree well with the previously published results. It verifies the reliability and accuracy of the present computer program.

In the next, the vibration and stability of the simply supported initially-stressed sandwich plates with FGM face sheets subjected to thermal loadings are investigated. The top and bottom FGM face sheet is made of silicon nitride and stainless steel, and is assumed to have the same thickness. The material properties of the constitutions of FGM face sheet are given as (Touloukian 1967, Javaheri and Eslami 2002)

Silicon nitride Si_3N_4 :

$$E = 322.22 \text{ Gpa}, \quad \alpha = 7.47 \times 10^{-6} / ^\circ\text{K}, \quad \kappa = 10.12 \text{ W/m}^\circ\text{K}, \\ \nu = 0.24, \quad \rho = 2370 \text{ kg/m}^3$$

Stainless steel SUS304:

$$E = 207.79 \text{ Gpa}, \quad \alpha = 15.32 \times 10^{-6} / ^\circ\text{K}, \quad \kappa = 12.14 \text{ W/m}^\circ\text{K}, \\ \nu = 0.317, \quad \rho = 8166 \text{ kg/m}^3$$

Parametric studies are conducted to examine the effects of various variables on the vibration and stability response of FGM/metal/FGM plates in thermal conditions. The non-dimensional vibration frequency ($\omega = \varpi b^2 \sqrt{\rho_M / h^2 E_M}$) and buckling load coefficient ($K_f = b^2 N_{xx} / E_M$) are defined and used throughout the study of vibration and stability problems. The positive buckling load coefficient K_f denotes that the initial axial stress is tensile. As $K_f = 0$ and $\beta = 0$, there exists no initial stresses. The absolute value of critical buckling load K_{cr} is the buckling load coefficient that causes the buckling.

Fig. 3 shows the effects of the metal layer thickness t_M and temperature rise ΔT on the vibration frequency of FGM/metal/FGM sandwich plates with $a/b = 1$, $a/h = 10$, $n = 1$, $\Delta T = \Delta T_1 = \Delta T_4$, $K_f = 0$, $\beta = 0$. ΔT_1 and ΔT_4 denote the temperature rise at $z = z_1$ and z_4 , respectively. As the temperature rise increases, the vibration frequency decreases regardless of the metal layer thickness. At a certain temperature rise, the critical temperature rise, the vibration frequency drops to zero and the plate vibration becomes unstable. As can be seen, the FGM/metal/FGM sandwich plate with a smaller metal layer thickness has a greater

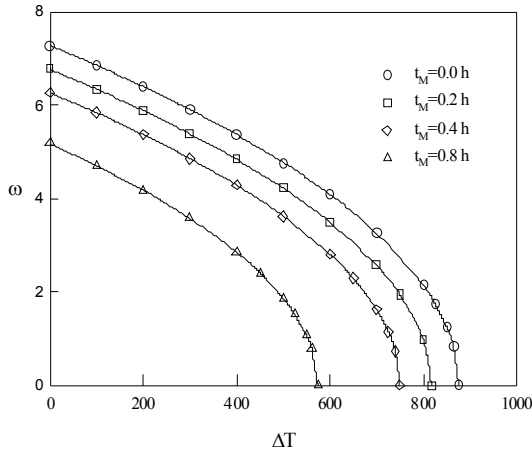


Fig. 3 Effect of temperature rise and metal layer thickness on the vibration frequency of sandwich plates ($a/b = 1, a/h = 10, n = 1, \Delta T = \Delta T_1 = \Delta T_4, K_f = 0, \beta = 0$)

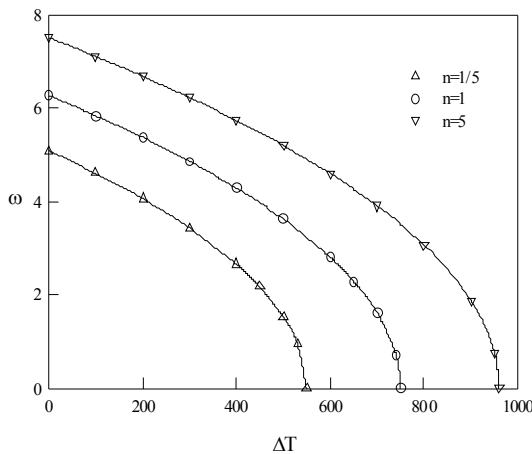


Fig. 4 Effect of temperature rise and volume fraction index on the vibration frequency of sandwich plates ($a/b = 1, a/h = 10, t_M = 0.4h, \Delta T = \Delta T_1 = \Delta T_4, K_f = 0, \beta = 0$)

Table 3 Effect of volume fraction index and metal layer thickness on the critical buckling temperature ($^{\circ}\text{C}$) of sandwich plates ($a/b = 1, a/h = 10, \Delta T_1 = \Delta T_4, K_f = 0, \beta = 0$)

t_M/h	n						
	0	1/5	1/2	1	2	5	∞
0	458.5	586.8	726.2	875.4	1031.9	1192.9	1361.3
0.2	458.5	569.7	689.9	817.1	948.7	1080.8	1209.8
0.4	458.6	549.3	647.2	749.8	855.1	960.1	1060.3
0.8	458.5	494.8	533.5	573.7	614.8	656.0	696.6

critical temperature rise. The vibration frequency reduces when the metal layer thickness increases for the plates under the same thermal loading. Like the temperature rise, the contribution of the metal layer thickness reduces the system stiffness of the plate. Thus, the sandwich plate with a larger metal layer thickness under a higher temperature rise has a smaller vibration frequency. As expected, the pure metal plate has the lowest vibration frequency and critical temperature rise as the metal layer thickness $t_M = h$. Fig. 4 shows the vibration frequencies of sandwich plates of $a/b = 1, a/h = 10, t_M = 0.4h, \Delta T = \Delta T_1 = \Delta T_4, K_f = 0, \beta = 0$ with different volume fraction indexes as a function of the temperature rise. The vibration frequency increases with the increasing volume fraction index, but reduces with the increasing temperature rise. Meanwhile, the FGM/metal/FGM sandwich plate with a larger volume fraction index has a higher critical temperature rise. It is attributable to the increase in the ceramic volume fraction along the plate thickness, which enhances the temperature-resistance ability of the sandwich plate. Table 3 presents the critical buckling temperatures of sandwich plates of $a/b = 1, a/h = 10, \Delta T_1 = \Delta T_4, K_f = 0, \beta = 0$ with various volume fraction indexes and metal layer thickness.

As can be seen, the FGM/metal/FGM plate with a larger volume fraction index and a smaller metal layer thickness has a larger critical buckling temperature. And the pure

Table 4 Effect of volume fraction index and metal layer thickness on the vibration frequency of sandwich plates under uniform temperature rise ($a/b = 1, a/h = 10, \Delta T = \Delta T_1 = \Delta T_4, K_f = 0, \beta = 0$)

ΔT	t_M/h	n						
		0	1/5	1/2	1	2	5	∞
0	0	4.5081	5.3650	6.2757	7.2781	8.4346	9.8662	11.8837
	0.2	4.5081	5.2311	5.9791	6.7665	7.6128	8.5458	9.6208
	0.4	4.5082	5.0842	5.6687	6.2647	6.8755	7.5028	8.1475
	0.8	4.5081	4.7291	4.9506	5.1710	5.3888	5.6025	5.8092
200	0	3.3848	4.3555	5.3421	6.3929	7.5733	9.0013	10.9763
	0.2	3.3848	4.2140	5.0385	5.8804	6.7629	7.7147	8.7896
	0.4	3.3847	4.0547	4.7122	5.3645	6.0180	6.6757	7.3390
	0.8	3.3848	3.6504	3.9142	4.1734	4.4262	4.6711	4.9048
400	0	1.1609	1.6925	2.2013	2.6607	3.0475	3.3410	3.5428
	0.2	1.1609	1.6269	2.0796	2.4986	2.8651	3.1593	3.3675
	0.4	1.1609	1.5457	1.9255	2.2862	2.6147	2.8962	3.1144
	0.8	1.1608	1.3174	1.4772	1.6365	1.7929	1.9435	2.0843

Table 5 Effect of volume fraction index and metal layer thickness on the vibration frequency of sandwich plates under nonuniform temperature rise ($a/b = 1, a/h = 10, \Delta T_4 = 0^\circ\text{C}, K_f = 0, \beta = 0$)

ΔT_1	t_M/h	n						
		0	1/5	1/2	1	2	5	∞
100	0	4.2552	5.1313	6.0558	7.0673	8.2278	9.6573	11.6637
	0.2	4.2553	4.9963	5.7584	6.5562	7.4095	8.3458	9.4199
	0.4	4.2553	4.8474	5.4454	6.0523	6.6715	7.3048	7.9531
	0.8	4.2551	4.4838	4.7130	4.9405	5.1650	5.3848	5.5968
200	0	3.9863	4.8864	5.8276	6.8499	8.0156	9.4437	11.4392
	0.2	3.9863	4.7499	5.5288	6.3390	7.2004	8.1409	9.2146
	0.4	3.9863	4.5983	5.2124	5.8320	6.4610	7.1013	7.7538
	0.8	3.9862	4.2243	4.4626	4.6987	4.9311	5.1579	5.3760
400	0	3.3849	4.3555	5.3421	6.3929	7.5733	9.0013	10.9763
	0.2	3.3850	4.2140	5.0385	5.8804	6.7629	7.7147	8.7896
	0.4	3.3849	4.0547	4.7122	5.3645	6.0180	6.6757	7.3390
	0.8	3.3848	3.6504	3.9142	4.1734	4.4262	4.6711	4.9048

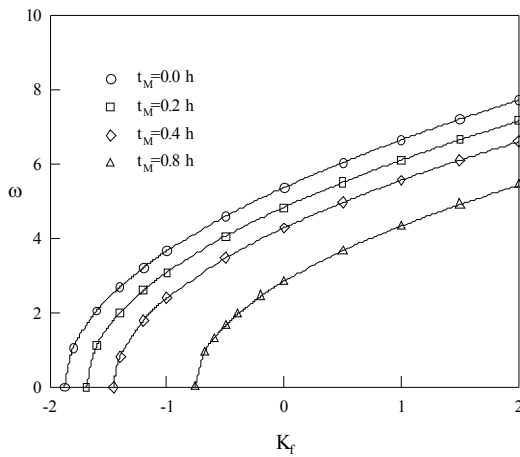


Fig. 5 Effect of buckling load coefficient and metal layer thickness on the vibration frequency of sandwich plates ($a/b = 1, a/h = 10, n = 1, \Delta T_1 = \Delta T_4 = 400^\circ\text{C}, \beta = 0$)

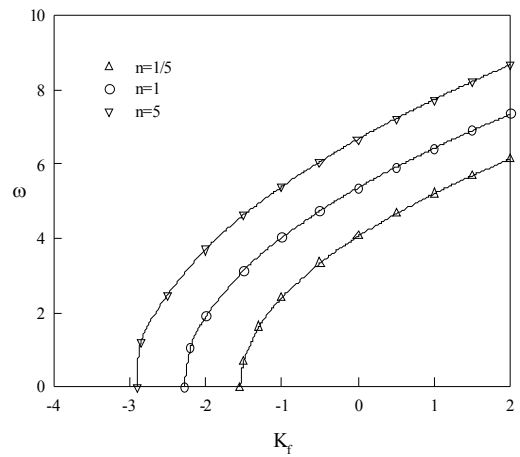


Fig. 6 Effect of buckling load coefficient and volume fraction index on the vibration frequency of sandwich plates ($a/b = 1, a/h = 10, t_M = 0.4h, \Delta T_1 = \Delta T_4 = 200^\circ\text{C}, \beta = 0$)

metal plate ($n = 0$) possesses a lowest critical buckling temperature. The effects of the volume fraction index and metal layer thickness on the vibration frequency of sandwich plates of $a/b = 1, a/h = 10, K_f = 0, \beta = 0$ under the uniform ($\Delta T_1 = \Delta T_4$) and nonuniform ($\Delta T_1 \neq \Delta T_4$) thermal loading are given in Tables 4 and 5, respectively. The vibration frequency increases with the increase in volume fraction index, but decreases as the metal layer thickness or temperature rise increases. However, the influence of volume fraction index on the variation of vibration frequency is more significant for the sandwich plate with a smaller metal core. Meanwhile, the vibration frequencies are not significantly affected by the increasing temperature rise for the sandwich plates subjected to the nonuniform temperature rise.

Fig. 5 presents the effects of the buckling load coefficient and metal layer thickness on the vibration frequency of sandwich plates with $a/b = 1, a/h = 10, n = 1,$

$\Delta T_1 = \Delta T_4 = 400^\circ\text{C}$ and $\beta = 0$. Fig. 6 shows the influence of the buckling load coefficient and volume fraction index on the vibration frequency of sandwich plates with $a/b = 1, a/h = 10, t_M = 0.4h, \Delta T_1 = \Delta T_4 = 200^\circ\text{C}$ and $\beta = 0$. The results reveal that the compressive load has a softening effect on the vibration frequency and the tensile load shows a reverse trend. As can be observed, the vibration frequency reduces with the decreasing buckling load coefficient and volume fraction index, but increases as the metal layer thickness decreases. When the buckling load coefficient continues to decrease to a certain value, the critical buckling load, the vibration frequency approaches to zero and the vibration is unstable. Tables 6 and 7 present the influence of the volume fraction index and metal layer thickness on the buckling load of sandwich plates with $a/b = 1, a/h = 10, \beta = 0$ subjected to the uniform and nonuniform temperature rise, respectively. Likewise, the buckling load increases with the increasing volume fraction index, but reduces with the

Table 6 Effect of volume fraction index and metal layer thickness on the buckling load of sandwich plates under uniform temperature rise ($a/b = 1, a/h = 10, \Delta T = \Delta T_1 = \Delta T_4, \beta = 0$)

ΔT	t_M/h	n						
		0	1/5	1/2	1	2	5	∞
0	0	2.0591	2.5681	3.0380	3.4487	3.7802	4.0139	4.1530
	0.2	2.0592	2.5069	2.9285	3.3083	3.6304	3.8767	4.0345
	0.4	2.0592	2.4303	2.7866	3.1179	3.4130	3.6582	3.8384
	0.8	2.0593	2.2111	2.3630	2.5124	2.6575	2.7959	2.9238
200	0	1.1609	1.6925	2.2013	2.6607	3.0475	3.3410	3.5428
	0.2	1.1609	1.6269	2.0796	2.4986	2.8651	3.1593	3.3675
	0.4	1.1608	1.5457	1.9255	2.2862	2.6147	2.8962	3.1144
	0.8	1.1609	1.3174	1.4772	1.6365	1.7929	1.9435	2.0843
400	0	0.2626	0.8170	1.3646	1.8728	2.3149	2.6680	2.9327
	0.2	0.2627	0.7468	1.2307	1.6888	2.0997	2.4419	2.7006
	0.4	0.2626	0.6611	1.0644	1.4546	1.8165	2.1341	2.3904
	0.8	0.2626	0.4238	0.5914	0.7606	0.9283	1.0911	1.2449

Table 7 Effect of volume fraction index and metal layer thickness on the buckling load of sandwich plates under nonuniform temperature rise ($a/b = 1, a/h = 10, \Delta T_4 = 0^\circ\text{C}, \beta = 0$)

ΔT	t_M/h	n						
		0	1/5	1/2	1	2	5	∞
100	0	1.8346	2.3492	2.8288	3.2517	3.5970	3.8457	4.0005
	0.2	1.8346	2.2869	2.7163	3.1059	3.4391	3.6974	3.8678
	0.4	1.8346	2.2091	2.5714	2.9100	3.2134	3.4677	3.6574
	0.8	1.8345	1.9877	2.1415	2.2934	2.4414	2.5828	2.7139
200	0	1.6100	2.1303	2.6196	3.0547	3.4139	3.6775	3.8479
	0.2	1.6101	2.0669	2.5040	2.9035	3.2478	3.5180	3.7010
	0.4	1.6101	1.9880	2.3561	2.7021	3.0138	3.2772	3.4764
	0.8	1.1600	1.7643	1.9201	2.0745	2.2252	2.3697	2.5041
400	0	1.1609	1.6925	2.2013	2.6607	3.0475	3.3410	3.5428
	0.2	1.1610	1.6269	2.0796	2.4986	2.8651	3.1593	3.3675
	0.4	1.1609	1.5457	1.9255	2.2862	2.6147	2.8962	3.1144
	0.8	1.1608	1.3174	1.4772	1.6365	1.7929	1.9435	2.0843

increasing metal layer thickness or temperature rise. Because the sandwich plate with a smaller metal layer thickness and higher volume fraction index has a higher stiffness, such a sandwich plate has a higher buckling load. As expected, the buckling loads for the sandwich plates without thermal effects are always higher than those of the sandwich plates under thermal loadings.

Table 8 presents the effect of the initial stress on the vibration frequencies of FGM/metal/FGM sandwich plates of $a/b = 1, a/h = 10, \beta = 0$ subjected to the temperature rise $\Delta T_1 = \Delta T_4 = 200^\circ\text{C}$. The initially compressive stressed sandwich plate with a higher metal layer thickness and lower volume fraction index has a lower vibration frequency than the corresponding initially tensile stressed sandwich plate. The effects of the bending stress ratio and volume fraction index on the vibration frequencies of initially stressed

FGM/metal/FGM sandwich plates with $a/b = 1, a/h = 10, t_M = 0.4h, n = 0.2, \Delta T = \Delta T_1 = \Delta T_4$ are presented in Table 9. It indicates that the bending stress produces a slight softening effect on the vibration frequency of the initially stressed sandwich plates with various layer thickness ratios. As the buckling coefficient approaches the critical buckling load, the effect of the bending stress on the vibration frequency is more significant, especially for the plates with a lower volume fraction index. The effects of the bending stress ratio and temperature rise on the vibration frequencies of initially stressed FGM/metal/FGM sandwich plates of $a/b = 1, a/h = 10, t_M = 0.4h, n = 0.2, \Delta T = \Delta T_1 = \Delta T_4$ are shown in Table 10. As can be seen, the bending stress has a significant influence on the vibration frequency of the sandwich plate subjected to a larger compressive initial stress and higher temperature rise.

Table 8 Effect of initial stress on the vibration frequency of sandwich plates ($a/b = 1, a/h = 10, \Delta T_1 = \Delta T_4 = 200^\circ\text{C}, \beta = 0$)

K_f	t_M/h	n						
		0	1/5	1/2	1	2	5	∞
1	0	4.6181	5.4935	6.4422	7.4986	8.7279	10.2603	12.4292
	0.2	4.6182	5.3548	6.1314	6.9584	7.8549	8.8518	10.0100
	0.4	4.6182	5.2035	5.8083	6.4316	7.0759	7.7430	8.4353
	0.8	4.6181	4.8415	5.0689	5.2971	5.5244	5.7485	5.9665
0	0	3.3848	4.3555	5.3421	6.3929	7.5733	9.0013	10.9763
	0.2	3.3848	4.2140	5.0385	5.8804	6.7629	7.7147	8.7896
	0.4	3.3847	4.0547	4.7122	5.3645	6.0180	6.6757	7.3390
	0.8	3.3848	3.6504	3.9142	4.1734	4.4262	4.6711	4.9048
-1	0	1.2602	2.7860	3.9463	5.0507	6.2077	7.5347	9.2991
	0.2	1.2603	2.6158	3.6303	4.5541	5.4565	6.3780	7.3699
	0.4	1.2603	2.4092	3.2669	4.0238	4.7292	5.4017	6.0470
	0.8	1.2598	1.7918	2.2247	2.6028	2.9435	3.2546	3.5377

Table 9 Effect of bending stress ratio on the vibration frequency of initially stressed sandwich plates ($a/b = 1, a/h = 10, t_M = 0.4h, \Delta T_1 = \Delta T_4 = 200^\circ\text{C}$)

$\frac{K_f}{K_{cr}}$	β	n						
		0	1/5	1/2	1	2	5	∞
0.9	0	4.6657	5.2490	5.8525	6.4753	7.1195	7.7873	8.4810
	20	4.6555	5.2398	5.8439	6.4671	7.1117	7.7796	8.4734
	40	4.6248	5.2118	5.8180	6.4427	7.0882	7.7567	8.4506
0.6	0	4.2816	4.8835	5.4987	6.1274	6.7723	7.4352	8.1182
	20	4.2767	4.8791	5.4947	6.1236	6.7686	7.4317	8.1147
	40	4.2618	4.8657	5.4824	6.1122	6.7577	7.4210	8.1041
0.3	0	3.8594	4.4882	5.1206	5.7586	6.4063	7.0657	7.7384
	20	3.8580	4.4870	5.1195	5.7576	6.4053	7.0648	7.7375
	40	3.8539	4.4834	5.1162	5.7546	6.4024	7.0620	7.7347
0	0	3.3847	4.0547	4.7122	5.3645	6.0180	6.6757	7.3390
-0.3	0	2.8321	3.5688	4.2648	4.9391	5.6030	6.2615	6.9165
	20	2.8303	3.5673	4.2635	4.9379	5.6019	6.2605	6.9155
	40	2.8247	3.5627	4.2596	4.9344	5.5986	6.2573	6.9124
-0.6	0	2.1410	3.0054	3.7647	4.4734	5.1546	5.8179	6.4665
	20	2.1312	2.9982	3.7588	4.4682	5.1498	5.8134	6.4621
	40	2.1012	2.9765	3.7409	4.4525	5.1354	5.7998	6.4488
-0.9	0	1.0710	2.3083	3.1870	3.9532	4.6633	5.3376	5.9827
	20	1.0257	2.2872	3.1712	3.9399	4.6514	5.3264	5.9720
	40	0.8757	2.2224	3.1233	3.8997	4.6154	5.2929	5.9395

Table 10 Effect of bending stress ratio on the vibration frequency of initially stressed sandwich plates in thermal environments ($a/b = 1, a/h = 10, t_M = 0.4h, n = 0.2, \Delta T = \Delta T_1 = \Delta T_4$)

$\frac{K_f}{K_{cr}}$	ΔT	β				$\frac{K_f}{K_{cr}}$	ΔT	β			
		0	10	20	40			0	10	20	40
0.9	0	6.0796	6.0776	6.0715	6.0475	-0.9	0	3.8389	3.8357	3.8262	3.7879
	100	5.6795	5.6774	5.6709	5.6451		100	3.1674	3.1636	3.1521	3.1054
	200	5.2490	5.2467	5.2398	5.2118		200	2.3083	2.3031	2.2872	2.2224
	300	4.7800	4.7774	4.7698	4.7391		300	0.7900	0.7745	0.7259	0.4847

6. Conclusions

The vibration and stability of initially stressed sandwich plates with FGM face sheets is investigated. The numerical analysis focuses on the vibration and buckling behaviors of the simply-supported initially-stressed FGM/metal/FGM plate under various thermal loadings. The critical buckling load and vibration frequency are apparently affected by the volume fraction index, temperature rise, initial stress and metal layer thickness. The vibration frequency and buckling load increases with the increase in the volume fraction index, but decreases with the increasing metal layer thickness and temperature rise. The critical buckling temperature increases when the volume fraction index increases and the metal layer thickness decreases. The compressive stresses significantly reduce the vibration frequency of sandwich plates and the tensile stresses have a reverse effect. The bending stress produces a slight softening effect on the vibration frequency. However, the bending stress has an apparent influence on the vibration frequency of the sandwich plate under a higher compressive stress and temperature rise.

References

- Brunell, E.J. and Robertson, S.R. (1974), "Initially stressed Mindlin plates", *AIAA J.*, **12**(1), 1036-1045.
- Chakravarty, S. and Pradhan, K.K. (2014), "Free vibration of exponential functionally graded rectangular plates in thermal environment with general boundary conditions", *Aeros. Sci. Tech.*, **36**(1), 132-156.
- Chen, C.S., Chen, T.J. and Chien, R.D. (2006), "Nonlinear vibration analysis of an initially stressed functionally graded plate", *Thin-Wall. Struct.*, **44**(8), 844-851.
- Chen, C.S., Fung, C.P. and Yu, S.Y. (2008), "Investigation on the vibration and stability of functionally graded plates", *J. Rein. Plast. Compos.*, **27**(13), 1435-1447.
- Chen, C.S., Hsu, C.Y. and Tzou, G.J. (2009), "Vibration and stability of functionally graded plates based on a higher-order deformation theory", *J. Rein. Plast. Compos.*, **28**(10), 1215-1234.
- Ghannadpour, S.A.M., Ovesy, H.R. and Nassirnia, M. (2012), "Buckling analysis of functionally graded plates under thermal loadings using the finite strip method", *Comput. Struct.*, **108-109**(1), 93-99.
- Javaheri, R. and Eslami, M.R. (2002), "Thermal buckling of functionally graded plates based on higher order theory", *J. Thermal Stress.*, **25**(7), 603-625.
- Kazerouni, S.M., Saidi, A.R. and Mohammadi, M. (2010), "Buckling analysis of thin functionally graded rectangular plates with two opposite edges simply supported", *Int. J. Eng., Tran. B: Appl.*, **23**(2), 179-192.
- Khalili, S.M.R. and Mohammadi, Y. (2012), "Free vibration analysis of sandwich plates with functionally graded face sheets and temperature-dependent material properties: A new approach", *Eur. J. Mech., A/Solids*, **35**(1), 61-74.
- Li, Q., Lu, V.P. and Kou, K.P. (2009), "Three-dimensional vibration analysis of functionally graded material plates in thermal environment", *J. Sound Vib.*, **324**(3-5), 733-750.
- Loja, M.A.R., Mota, S.C.M. and Barbosa, J.I. (2013), "Analysis of functionally graded sandwich plate structures with piezoelectric skins, using B-spline finite strip method", *Compos. Struct.*, **96**(1), 606-615.
- Mahi, A., Bedia, E.A.A. and Benkhedda, A. (2013), "Free vibration analysis of FGM plates under initial thermal stresses", *Adv. Mater. Res.*, **682**(1), 49-56.
- Malekzadeh, P., Shahpari, S.A. and Ziaee, H.R. (2010), "Three-dimensional free vibration of thick functionally graded annular plates in thermal environment", *J. Sound Vib.*, **329**(4) 425-442.
- Matsunaga, H. (2005), "Thermal buckling of cross-ply laminated composite and sandwich plates according to a global higher order deformation theory", *Compos. Struct.*, **68**(1), 439-454.
- Matsunaga, H. (2009), "Thermal buckling of functionally graded plates according to a 2D higher-order deformation theory", *Compos. Struct.*, **90**(1), 76-86.
- Natarajan, S., Baiz, P.M., Ganapathi, M., Kerfriden, P. and Bordas, S. (2011), "Linear free flexural vibration of cracked functionally graded plates in thermal environment", *Comput. Struct.*, **89**(15-16), 1535-1546.
- Pradyumna, S. and Bandyopadhyay, J.N. (2010), "Free vibration and buckling of functionally graded shell panels in thermal environments", *Int. J. Struct. Stab. Dyn.*, **10**(5), 1031-1053.
- Rahimabadi, A.A., Natarajan, S. and Bordas, S.P.A. (2013), "Vibration of functionally graded material plates with cutouts & cracks in thermal environment", *Key Eng. Mater.*, **560**, 157-180.
- Shafiee, A.A., Daneshmand, F., Askari, E. and Mahzoon, M. (2014), "Dynamic behavior of a functionally graded plate resting on Winkler elastic foundation and in contact with fluid", *Struct. Eng. Mech., Int. J.*, **50**(1), 53-71.
- Shariat, B.A.S. and Eslami, M.R. (2007), "Buckling of thick functionally graded plates under mechanical and thermal load", *Compos. Struct.*, **78**(3), 433-439.
- Shen, H.S. and Li, S.R. (2008), "Postbuckling of sandwich plates with FGM face sheets and temperature-dependent properties", *Compos.: Part B Engng.*, **39**(2), 332-344.
- Shen, H.S. and Zhu, Z.H. (2010), "Buckling and postbuckling behavior of functionally graded nanotube-reinforced composite plates in thermal environments", *Comput. Mater. Continua*, **18**(2), 155-182.
- Shi, P. and Dong, C.Y. (2012), "Vibration analysis of functionally graded annular plates with mixed boundary conditions in thermal environment", *J. Sound Vib.*, **331**(15), 3649-3662.
- Touloukian, Y.S. (1967), *Thermophysical Properties of High Temperature Solid Materials*, McMillan Co., New York, USA.
- Yang, J. and Shen, H.S. (2003), "Nonlinear analysis of functionally graded plates under transverse and in-plane loads", *Int. J. Non-Linear Mech.*, **38**(4), 467-482.
- Zhao, X., Lee, Y.Y. and Liew, K.M. (2009), "Mechanical and thermal buckling analysis of functionally graded plates", *Compos. Struct.*, **90**(2), 161-171.

CC